The α and β structural forms of poly(tetramethylene terephthalate): a study by broad line nuclear magnetic resonance

I. S. Davidson*, A. J. Manuel and I. M. Ward
Department of Physics, University of Leeds, Leeds LS2 9JT, UK
(*Received* 8 *March* 1982)

Broad line nuclear magnetic resonance measurements have been carried out on oriented poly(tetramethylene terephthalate). The second moment was determined as a function of specimen orientation for the polymer in its unstrained state, and also under extension, where previous X-ray diffraction measurements have shown that the crystal structure changes from the α form (relaxed) to the β form (strained). The n.m.r. results for the stretched specimen are consistent with the molecular conformation being close to full extension, and agree quantitatively with the crystal structure proposed by Hall and Pass. The n.m.r. results for the unstrained material are, however, not in agreement with any of the crystal structures which have been proposed and suggest that, contrary to present conclusions, the conformation and orientation of the central methylene pairs in the glycol residue must remain substantially unchanged in the transformation from the α to the β form.

Keywords Poly(tetramethylene terephthalate); nuclear magnetic resonance measurements; broad line; specimen orientation; second moment; α form; β form

INTRODUCTION

There has been considerable interest in the structure and properties of oriented poly(tetramethylene terephthalate), 4GT. Much of the interest stems from the observation that when the oriented polymer is extended there is a marked change in the X-ray diffraction pattern, which indicates that the crystalline regions are being transformed from one crystalline structure to a new structure[1-3]. The structure at high extension has been termed the β form and it appears that the molecular chain in this structure is close to its fully extended length. The structure in the relaxed state is termed the α form and in this case the molecular chain is $\sim 10\%$ shorter than in the β form. It has been shown by X-ray and Raman spectroscopy measurements[3,4] that these changes in the crystal structure on deformation are completely reversible, although some hysteresis effects can be observed[4]. Detailed X-ray structural studies have been undertaken on the α and β forms by Hall and co-workers[6-7], by Yokouchi and co-workers[9] and by Stambaugh and co-workers[10,11].

It appears that the transformation from the α to the β form occurs primarily by a discontinuous change in the conformation of the glycol residue.

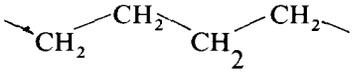

With regard to the details of the α and β structures, however, the situation is at present not so clear. Although the evidence from infra-red and Raman spectroscopy[12] suggests that the extended β structure is close to a fully *trans–trans–trans* sequence in the glycol residue, there are significant departures from this simple form in the crystal structures proposed by Hall and co-workers[6-8] and by Yokouchi and co-workers[9] which are themselves significantly different. In fact the latter workers suggest a near eclipsed conformation for the glycol residue. It appears that the contracted α form approaches a *gauche–trans–gauche* sequence. Although this is again consistent with the spectroscopic evidence there are differences in detail between the structure proposed by Mencik[5], which is supported by Stambaugh and co-workers[10,11], and that of Desborough and Hall[7] which is in close agreement with that of Yokouchi and co-workers[9].

A major problem in the interpretation of the X-ray diffraction data concerns the relative weighting to be given to the intensities of different diffraction spots. This relates directly to the scattering function of the different atoms and because of the comparatively low contribution of the hydrogen atoms the X-ray technique is not especially suitable for defining the conformation of the glycol residue. In this respect wide line nuclear magnetic resonance (n.m.r.) is complementary, because the line shape in solid materials arises from dipolar interaction between nuclear magnetic moments of the nuclei, in this case, protons. Studies of the anisotropy of the n.m.r. signal in oriented polymers therefore offer a possible way of examining critically the proposed models for the structure of 4GT. In this paper we will present results for both the stretched and relaxed material and compare the observed n.m.r. anisotropy with that predicted by various proposed structures.

THEORY

The anisotropy of the n.m.r. second moments can, in general, be expressed in terms of spherical harmonic functions of the polar and azimuthal angles (γ,φ_γ), relating

* Now at British Nuclear Fuels, Springfields Works, Preston, PR4 OXJ

0032-3861/83/010030-07$03.00

the direction of the applied magnetic field to the specimen orientation axes[13]. For transversely isotropically oriented materials the spherical harmonic functions reduce to Legendre polynomials of argument $\cos\gamma$ as discussed originally by McBrierty and Ward[14]. For partially crystalline specimens McBrierty and Ward introduced the concept of transversely isotropic structural units which permitted the description of the orientation by a distribution function $f(\Delta)$ defined such that $f(\Delta)\sin\Delta d\Delta$ represents the fraction of structural units whose symmetry axes lie at angles between Δ and $\Delta+d\Delta$ with respect to the specimen symmetry axis, or draw direction. This orientation function may be expanded in Legendre polynomials.

$$f(\Delta)=\sum_{l=0}^{\infty} b_l P_l(\cos\Delta) \tag{1}$$

where b_l may be shown to be equal to $(l+\frac{1}{2})\overline{P_l(\cos\Delta)}$ where $\overline{P_l(\cos\Delta)}$ is the average value over the distribution.

The corresponding anisotropy of the wide line n.m.r. second moment, $\langle\Delta H^2\rangle$, as a function of the angle γ between the applied magnetic field and the draw direction of the specimen may be written:

$$\langle\Delta H^2\rangle=\sum_{l=0,2,4} A_l P_l(\cos\gamma) \tag{2}$$

where

$$A_0=\frac{4}{5}G\sqrt{4\pi}S_{00}\overline{P_0(\cos\Delta)} \tag{3a}$$

$$A_2=\frac{8}{7}G\sqrt{\frac{4\pi}{5}}S_{20}\overline{P_2(\cos\Delta)} \tag{3b}$$

$$A_4=\frac{72}{35}G\sqrt{\frac{4\pi}{9}}S_{40}\overline{P_4(\cos\Delta)} \tag{3c}$$

and $G=\frac{3}{2}I(I+1)g^2\mu_n{}^2$, I is the nuclear spin quantum number, g the nuclear spectroscopic splitting factor and μ_n the nuclear magneton. The lattice sums S_{lm} which characterize the structural units of the material and which may be calculated from the structure determined by X-ray diffraction are given by:

$$S_{lm}=\frac{1}{N}\sum_{j>k}^{N} r_{jk}^{-6} Y_{lm}^{*}(\theta_{jk},\varphi_{jk}) \tag{4}$$

In this expression r_{jk} is the length of the internuclear vector between the jth and kth nucleus and θ_{jk} and φ_{jk} are the polar and azimuthal angles specifying the orientation of $\mathbf{r}_{jk}$ in the crystalline lattice.

For transversely isotropic structural units only S_{l0} are non-zero, and the spherical harmonics in equation (4) may be reduced to Legendre polynomials $P_l(\cos\theta_{jk})$.

It is convenient to calculate the S_{lm} using the r_{jk} in Å. The value of G in the equation (3) for the A_l is then replaced by $10^{48}G=895{\cdot}5$ for $\langle\Delta H^2\rangle$ in equation (2) in gauss[2]. The A_l can then be written:

$$A_0=2540\,S_{00}\overline{P_0(\cos\Delta)} \tag{5a}$$

$$A_2=1622\,S_{20}\overline{P_2(\cos\Delta)} \tag{5b}$$

$$A_4=2177\,S_{40}\overline{P_4(\cos\Delta)} \tag{5c}$$

Using the A_l calculated from the experimental variation of $\langle\Delta H^2\rangle$ with γ using equation (2) and the S_{l0} calculated for models proposed on the basis of X-ray diffraction measurements the values of $\overline{P_l(\cos\Delta)}$ and $\overline{\cos^l\Delta}$ for $l=0,2,4$ can be derived. These quantities are then a guide to the validity of the proposed models for the structure of the polymer.

EXPERIMENTAL

Preparation of samples

The samples were in the form of oriented tape 20 μm thick and 1.2 mm wide, which had been prepared by melt spinning and drawing, followed by an annealing treatment. First, 4GT polymer was prepared with a molecular weight characterized by a relative viscosity of 2.2, determined in a 1% solution in *o*-chlorophenol at 25°C. The polymer was melt-extruded at 280°C through a rectangular die and immediately quenched into water at ambient temperature. The resultant isotropic tape was drawn between rollers moving at different speeds over a heated cylinder at 90°C and a heated plate at 160°C to a draw ratio of 5:1. The oriented tape was subsequently annealed at constant length for 20 h at 200°C in a vacuum oven.

The oriented annealed tape was shown by X-ray diffraction to have well developed crystallinity and high crystalline orientation. Previous work[15] has shown that such samples are ~40% crystalline, based on density measurements and a crystalline density of 1.39 g cm^{-3}.

Two samples of 4GT were prepared for n.m.r. measurement by winding the tape on to a former and cutting off the curved ends to give a bundle of parallel fibres. This was a straightforward process in the preparation of sample (A), the α 4GT specimen. Sample (B), the β 4GT specimen was made by winding a single long piece of tape on to a thin flat copper plate while the tape was under a constant load of 200 g. Tests on 10 pieces of tape from the same batch showed this gave an extension of 8% ± 2%. The wound sample was then mounted in a jig, cooled in liquid nitrogen and machined while in a liquid nitrogen bath. In this way the ends of the specimen could be cut away to leave a bundle of strained fibres in the n.m.r. probe. During the series of measurements made on the β 4GT specimen, the n.m.r. probe was maintained at or below liquid nitrogen temperature in order to keep the sample in its glassy state and so maintain the strained condition.

N.m.r. measurements

The n.m.r. measurements were made using the 30 mHz *Q* meter apparatus and cryostat described by Davenport and Manuel[16], which now incorporates an improved low noise r.f. pre-amplifier. Once the optimum r.f. level required by the main amplifier/detector circuit had been determined, the r.f. power to the sample was adjusted so that it was well below the power level which produced saturation. A magnetic field modulation of amplitude 0.5 Gauss was used on sample (A) giving an Andrew[17] correction of 0.06 Gauss[2] and a modulation of amplitude 0.84 Gauss used on sample (B) giving an Andrew

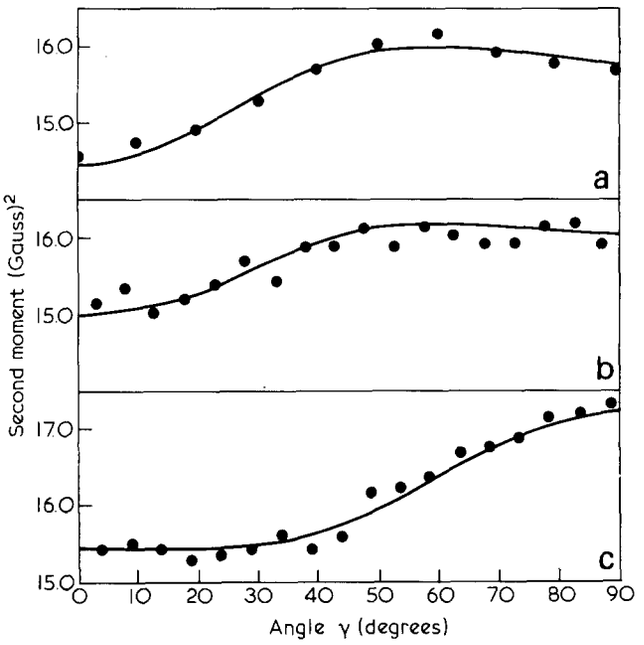

Figure 1 Anisotropy of n.m.r. second moment in oriented 4GT. (a) α 4GT specimen A (b) α 4GT specimen B (c) β 4GT specimen B strained 8%

correction of 0.18 Gauss^2. These corrections have been applied to all the results described here.

Each signal was obtained using a signal averager, sampling at a field interval of 0.05 Gauss, to sum over 16 sweeps. To circumvent the problem of field drift during the averaging process the signal from a small sample of liquid fluorocarbon fixed next to the cryostat was used to initiate the data collection process, thus synchronizing the recorded signal to the applied magnetic field. During the accumulation of signals in the signal averager, the temperature remained constant to within 0.05 K. All the measurements were made in temperature range 6–7 K.

The averaged signal accumulated in the signal averager was output to a paper tape punch and then fed into the University main frame computer where the second moment was calculated.

The variation of $\langle \Delta H^2 \rangle$ as a function of the angle between the applied field and fibre direction (γ) was measured for three cases:

(1) sample (A), relaxed α 4GT,

(2) sample (B), strained β 4GT, prepared by winding under tension,

(3) sample (B), relaxed α 4GT, prepared by allowing the strained sample to warm up to room temperature and so relax back to α 4GT.

The initial measurements were made on sample (A) for values of γ at about 10° intervals over a range of 360°. All subsequent measurements were made on sample (B) for values of γ at 5° intervals over a range of γ from −15° to +105°. For this sample, 3 averaged signals were taken at each orientation yielding 3 values of $\langle \Delta H^2 \rangle$. The mean $\langle \Delta H^2 \rangle$ was taken as the measured second moment for that particular orientation.

RESULTS

The measured values of $\langle \Delta H^2 \rangle$ (corrected for modulation and sweep rate effects) for the two relaxed samples and one strained sample of 4GT over the range of γ 0–90° are shown in *Figure 1*, each with a curve representing the least squares fit of equation (2) to the experimental points. The resulting coefficients, A_l, of equation (2) are given for all three specimens in *Table 1*.

Previously published data from X-ray diffraction work[5–11] enabled equation (4) to be used to calculate the lattice sums, S_{l0}, for each of the molecular models put forward to date. The results of these calculations are given in *Tables 2* and *3*. To test the validity of each model, equations (3b) and (3c) were then used to calculate $\overline{P_2(\cos\Delta)}$ and $\overline{P_4(\cos\Delta)}$ and hence $\overline{\cos^2\Delta}$ and $\overline{\cos^4\Delta}$ for sample B since more accurate values of A_0, A_2 and A_4 had been determined for this sample. The results are summarized in *Table 2* for the relaxed form (α 4GT) and in *Table 3* for the strained form (β 4GT).

Not all workers have quoted hydrogen coordinates for their models and there is variation in the C–H bond lengths used amongst those who have. In our calculation of the lattice sums, we have used published hydrogen coordinates whenever possible or derived them from published conformational data or from published carbon coordinates by assuming the normal tetrahedral bond angle and C–H bond lengths of 1.07 Å for aromatic bonds and 1.09 Å for paraffinic bonds. Although the value chosen for the length of the C–H bonds will strongly affect the magnitude of the lattice sums, it will have little effect on the signs of S_{20} and S_{40} as they are functions of the $\cos\theta_{jk}$, where the θ_{jk} are the angles between the interproton vectors and the 'c' axis of the unit cell.

Thus, it should still be possible to identify the best model as long as all the models considered have dissimilar conformations.

DISCUSSION

Strained (β) 4GT

Table 3 shows the values of $\overline{\cos^2\Delta}$ and $\overline{\cos^4\Delta}$ derived from the n.m.r. measurements and the postulated crystal structures. Although the model of Yokouchi *et al.* gives a very high $\overline{\cos^2\Delta}$ the remaining values are reasonable for an oriented specimen of draw ratio 5:1[18] and none of the models could be eliminated on the basis of these values. However, the Desborough–Hall refined models produced values of S_{20} and S_{40} very similar to those derived from the Pass–Hall model 6, which would make it very difficult to distinguish between them. We therefore decided that

Table 1 Coefficients of legendre polynomials from the best least squares fit of the experimental points to equation (2)

	Relaxed (α) 4GT		
	A_0	A_2	A_4
Sample A relaxed specimen	15.690 (±0.185)	−0.578 (±0.362)	−0.697 (±0.431)
Sample B strained material that had been allowed to relax	15.978 (±0.014)	−0.517 (±0.031)	−0.440 (±0.036)
	Strained (β) 4GT		
	A_0	A_2	A_4
Sample B strained specimen	16.365 (±0.036)	−1.356 (±0.030)	0.467 (±0.076)

Table 2 Lattice sums S_{l0} calculated for the models proposed for α 4GT. Values of $\overline{P_l(\cos\Delta)}$ derived from equations (5) using these S_{l0} and the experimental values of $A_0 = 15.978, A_2 = -0.517$ and $A_4 = -0.440$ from *Table 1*. Values of $\overline{\cos^2\Delta}$ and $\overline{\cos^4\Delta}$ calculated from the $P_l(\cos\Delta)$ and the definition of Legendre polynomials

Model	$10^3 S_{00}$	$10^3 S_{20}$	$10^3 S_{40}$	$\overline{P_0(\cos\Delta)}$	$\overline{P_2(\cos\Delta)}$	$\overline{P_4(\cos\Delta)}$	$\overline{\cos^2\Delta}$	$\overline{\cos^4\Delta}$
α 4GT Hall-Pass 1	+7.360	+0.237	−1.136	+0.855	−1.345	+0.178	−0.563	−0.528
α 4GT Hall-Pass 2	+7.420	+0.229	−1.111	+0.848	−1.392	+0.182	−0.595	−0.554
α 4GT Hall-Pass 3	+7.300	+0.190	−0.741	+0.862	−1.678	+0.273	−0.785	−0.696
α 4GT Hall-Pass 4	+7.345	+0.169	−0.644	+0.856	−1.886	+0.314	−0.924	−0.806
α 4GT Yokouchi	+6.644	+0.368	−1.505	+0.947	−0.866	+0.134	−0.244	−0.264
α 4GT Mencik	+6.265	+0.284	−1.070	+1.004	−1.122	+0.189	−0.415	−0.398
α 4GT Stambaugh-Koenig-Lando	+6.522	+0.171	−1.318	+0.965	−1.864	+0.153	−0.909	−0.830
α 4GT Desborough-Hall 5 (Yokouchi, refined 1)	+6.505	+0.099	−2.275	+0.967	−3.220	+0.089	−1.813	−1.619
α 4GT Desborough-Hall 6 (Yokouchi, modified and refined)	+6.231	+0.460	−0.865	+1.010	−0.693	+0.234	−0.129	−0.143

Table 3 Lattice sums S_{l0} calculated for the models proposed for β 4GT. Values of $\overline{P_l(\cos\Delta)}$ derived from equations (5) using these S_{l0} and the experimental values of $A_0 = 16.365, A_2 = -1.356$ and $A_4 = 0.467$ from *Table 1*. Values of $\overline{\cos^2\Delta}$ and $\overline{\cos^4\Delta}$ calculated from the $P_l(\cos\Delta)$ and the definition of Legendre polynomials

Model	$10^3 S_{00}$	$10^3 S_{20}$	$10^3 S_{40}$	$\overline{P_0(\cos\Delta)}$	$\overline{P_2(\cos\Delta)}$	$\overline{P_4(\cos\Delta)}$	$\overline{\cos^2\Delta}$	$\overline{\cos^4\Delta}$
β 4GT Hall-Pass 6	+8.180	−3.380	+3.450	+0.788	+0.247	+0.062	+0.498	+0.356
β 4GT Hall-Pass 7	+8.246	−2.629	+0.600	+0.781	+0.318	+0.358	+0.545	+0.463
β 4GT Yokouchi	+5.908	−0.810	−0.689	+1.091	+1.032	−0.311	+1.021	+0.719
β 4GT Desborough-Hall 3 (Hall-Pass, modified 1)	+7.659	−2.081	+3.193	+0.841	+0.402	+0.067	+0.601	+0.445
β 4GT Desborough-Hall 4 (Hall-Pass, modified 2)	+7.587	−1.789	+2.642	+0.849	+0.467	+0.081	+0.645	+0.486
β 4GT Desborough-Hall 5 (Yokouchi, reindexed)	+7.690	−3.454	+2.522	+0.838	+0.242	+0.085	+0.495	+0.358

only the Pass–Hall models 6 and 7 and the model of Yokouchi *et al.* need be further analysed.

In order to determine which model best fitted the n.m.r. results, the experimental second moment anisotropy was compared with the anisotropy predicted from these three remaining models. As small changes in the interpair proton distance, caused by uncertainty in the C–H bond length, greatly affect the calculated value of the second moment the calculated anisotropy was scaled so that it could be compared with the measured anisotropy. This was done by using a scaling factor to make the calculated isotropic component equal to the measured isotropic component. Furthermore since it is not possible to calculate the second moment of the amorphous fraction, it was assumed that this was equal to the measured isotropic component of the sample. Using the degree of crystallinity as an additional adjustable parameter the best fit of the above three models to the experimental results was obtained using a least squares fitting procedure. The resulting curves are shown in *Figure 2* together with the experimental results. It is clear that only the curve for the Hall–Pass model 7 is in agreement with the measured results, and this agreement is excellent with a reasonable value for the crystallinity.

Figure 3 shows the conformation of each of the three models considered. The two Hall–Pass models differ only slightly and yet the predicted anisotropy of all three models is markedly different. This behaviour can be explained by considering *Table 6* which shows the intrachain contributions to the lattice sums from each of

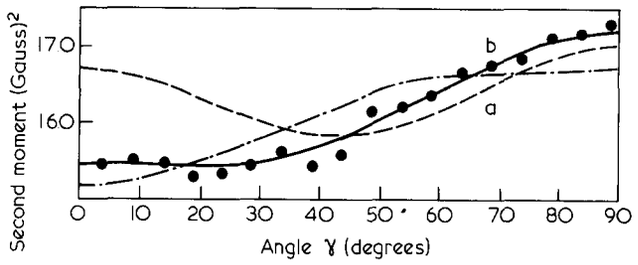

Figure 2 Anisotropy of n.m.r. second moment in β 4GT (specimen B) and the best least squares fit of the anisotropy predicted from (a) Hall-Pass model 6, 18% crystallinity (b) Hall-Pass model 7, 40% crystallinity (c) Yokouchi model, 37% crystallinity

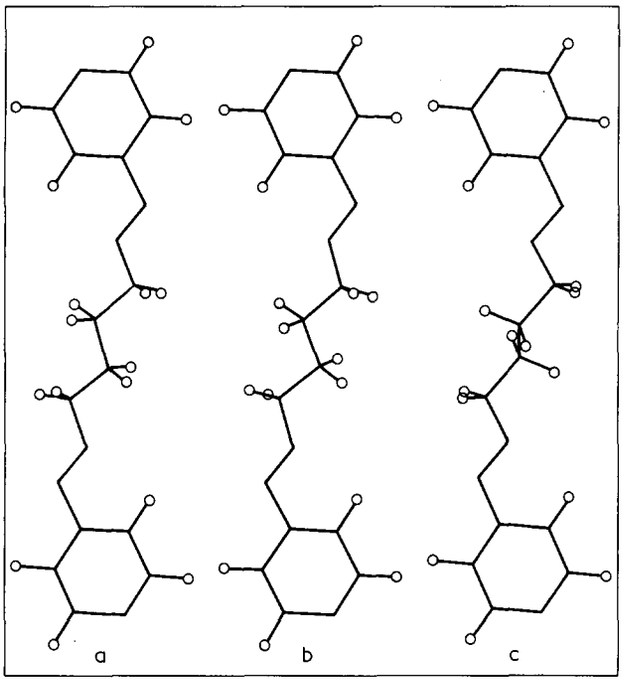

Figure 3 Conformation diagrams for three models of β 4GT considered. (○) Positions of hydrogen atoms. (a) Hall-Pass model 6 (b) Hall-Pass model 7 (c) Yokouchi model

the non-equivalent nuclei in the unit cell.

This data shows that it is the methylene pair interactions which dominate the lattice sums and, furthermore, that the differences in predicted n.m.r. anisotropy arise in the contribution from the central methylene pair, the other contributions being of the same order in all 3 models.

Hall–Pass models 6 and 7, although very similar in conformation, show a large discrepancy in the S_{40} contribution. S_{40} is a function of $P_4(\cos\theta_{jk})$, where θ_{jk} is the angle between the vector joining the jth and kth nuclei and the crystal c axis. From *Figure 5* it can be seen that this function is very sensitive to small changes in θ_{jk} for the values of θ_{jk} predicted in the centre of the methylene chain (see *Table 6*).

The major difference between the Hall–Pass models and the Yokouchi model is in the S_{20} contribution of the central methylene pair. This is a function of $P_2(\cos\theta_{jk})$, which is another rapidly changing function of θ_{jk} (see *Figure 5*) for the values of θ_{jk} found in this region of the molecule (see *Table 6*).

This qualitative argument describes the wide variation in calculated second moment anisotropy of the postulated conformational models, which indicates model 7 by Hall and Pass to be identified as the best model of β4GT.

Relaxed (α) 4GT

Figures 1a and *b* show that the second moment anisotropy curves measured on two different samples are in good agreement with each other.

The values of A_2 in *Table 1*, derived by fitting equation (2) to the *Figures 1a* and *b*, are negative and the values of the S_{20} in *Table 2* calculated for all the models considered are positive. This means that the corresponding values of $P_2(\cos\Delta)$ calculated from equation (3b) are negative for all the models ($\cos^2\Delta < 0.33$), which is physically unreasonable for a sample of draw ratio $\lambda = 5$ on an affine deformation model[18]. Furthermore the values of both $\overline{\cos^2\Delta}$ and $\overline{\cos^4\Delta}$ deduced are inconsistent with the values obtained for the same material in the β phase. It therefore follows that all the models for the α phase are unsatisfactory in respect of the fact that they predict positive values of S_{20}, whereas negative values would be required to give physically reasonable values of the orientation functions. Consequently the problem must be in the structure giving rise to positive values of S_{20}.

The interchain and intrachain contributions to the total lattice sums for α 4GT are shown in *Table 4*. The data in *Table 4* show that although the interchain contributions are negative for all models the intrachain contributions all have sufficiently large positive values to make the overall values of the S_{20} positive. Further examination of individual proton pair contributions has not shown any anomalous atomic separations which could affect this result.

As in the β material, the intrachain lattice sums are dominated by the methylene pair interactions and since S_{20} is a function of $P_2(\cos\theta_{jk})$, it can be seen from *Figure 5* and the conformational diagrams in *Figure 4* that the outer methylene pair will only give rise to a small negative S_{20} contribution. It is the central methylene pairs

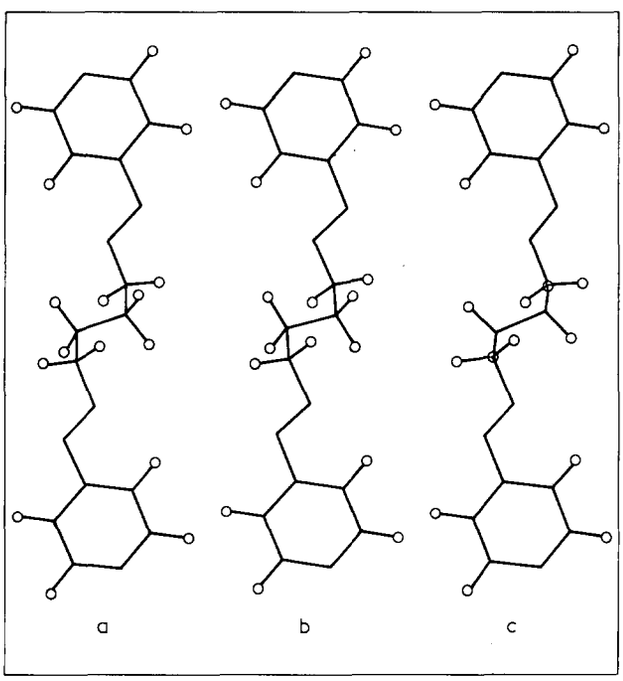

Figure 4 Conformation diagrams for three models of α 4GT considered. (○) Positions of hydrogen atoms (a) Hall-Pass model 1 (b) Yokouchi model (c) Mencik model

Table 4 Lattice sums S_{l0} and the contributions from intrachain interactions ($S_{l0}^{(1)}$) and interchain interactions ($S_{l0}^{(2)}$) for α 4GT. $S_{l0} = S_{l0}^{(1)} + S_{l0}^{(2)}$

	Lattice sums			Intrachain contribution			Interchain contribution		
Model	$10^3 S_{00}$	$10^3 S_{20}$	$10^3 S_{40}$	$10^3 S_{00}^{(1)}$	$10^3 S_{20}^{(1)}$	$10^3 S_{40}^{(1)}$	$10^3 S_{00}^{(2)}$	$10^3 S_{20}^{(2)}$	$10^3 S_{40}^{(2)}$
α 4GT Hall-Pass 1	+7.360	+0.237	−1.136	+5.903	+0.635	−0.784	+1.457	−0.398	−0.352
α 4GT Hall-Pass 2	+7.420	+0.229	−1.111	+5.966	+0.622	−0.755	+1.454	−0.393	−0.356
α 4GT Hall-Pass 3	+7.300	+0.190	−0.741	+5.876	+0.530	−0.336	+1.424	−0.340	−0.405
α 4GT Hall-Pass 4	+7.345	+0.169	−0.644	+5.929	+0.505	−0.237	+1.416	−0.336	−0.407
α 4GT Desborough-Hall 5 (Yokouchi refined)	+6.505	+0.099	−2.275	+4.697	+0.376	−1.639	+1.808	−0.277	−0.636
α 4GT Desborough-Hall 6 (Yokouchi modified and refined)	+6.231	+0.460	−0.865	+4.520	+0.662	−0.198	+1.711	−0.202	−0.667
α 4GT Yokouchi	+6.644	+0.368	−1.505	+4.865	+0.715	−0.958	+1.779	−0.347	−0.547
α 4GT Mencik	+6.265	+0.284	−1.070	+4.253	+0.810	−0.505	+2.012	−0.526	−0.565
α 4GT Stambaugh-Koenig-Lando	+6.528	+0.165	−1.335	+4.603	+0.639	−0.806	+1.925	−0.474	−0.529

Table 5 Lattice sums S_{l0} and the contributions from intrachain interactions ($S_{l0}^{(1)}$) and interchain interactions ($S_{l0}^{(2)}$) for β 4GT. $S_{l0} = S_{l0}^{(1)} + S_{l0}^{(2)}$

	Lattice sums			Intrachain contributions			Interchain contributions		
Model	$10^3 S_{00}$	$10^3 S_{20}$	$10^3 S_{40}$	$10^3 S_{00}^{(1)}$	$10_3 S_{20}^{(1)}$	$10^3 S_{40}^{(1)}$	$10^3 S_{00}^{(2)}$	$10_3 S_{20}^{(2)}$	$10^3 S_{40}^{(2)}$
β 4GT Hall-Pass 6	+8.180	−3.380	+3.450	+5.928	−3.413	+3.525	+2.252	+0.033	−0.075
β 4GT Hall-Pass 7	+8.246	−2.629	+0.600	+6.117	−2.791	+1.205	+2.129	+0.162	−0.605
β 4GT Desborough-Hall 3 (Hall-Pass modified 1)	+7.659	−2.081	+3.193	+4.811	−2.313	+2.460	+2.848	+0.232	+0.733
β 4GT Desborough-Hall 4 (Hall-Pass modified 2)	+7.587	−1.789	+2.642	+4.767	−2.252	+2.038	+2.820	+0.463	+0.604
β 4GT Desborough-Hall 5 (Yokouchi reindexed)	+7.690	−3.454	+2.522	+4.816	−1.808	+1.030	+2.874	−1.646	+1.492
β 4GT Yokouchi	+5.908	−0.810	−0.689	+4.662	−0.516	−0.376	+1.246	−0.294	−0.313

which are the origin of the positive S_{20} because they are at a much more acute angle to the '*c*' axis in all the postulated models. Therefore, it is the central region of the chain which is not compatible with the n.m.r. results in the models discussed.

An estimate of values of S_{20} and S_{40} for a possible conformation in α 4GT can be made by assuming that the measured orientation functions $\overline{P_2(\cos\Delta)}$ and $\overline{P_4(\cos\Delta)}$ remain the same on transition between α and β phase 4GT. From the X-ray work of Brereton *et al.*[4], it appears that this is a good approximation, the orientation in the β phase being reported as only slightly less than in the α phase. By substituting the values of A_2 and A_4 measured on α 4GT and the calculated values of $\overline{P_4(\cos\Delta)}$ and $\overline{P_4(\cos\Delta)}$ from β 4GT into equations (5b) and (5c), it follows that both S_{20} and S_{40} would be negative. This means that the dominant interpair vectors must lie between 55° and 70° to the crystal '*c*' axis, as in the best fitting model of β 4GT.

This implies that both the conformation and orientation of the central methylene pairs in the glycol residue do not change radically on transforming from α to β 4GT and that changes in conformation of the terephthaloyl residue

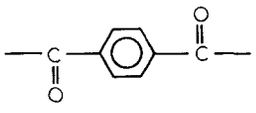

of the molecule must also contribute to the measured increase in repeat distance on α to β phase transitions.

Table 6 Individual non-equivalent hydrogen nuclei contributions $S_{l0}^{(3)}$ to the intrachain part of the lattice sums for β 4GT. The intrachain contribution is obtained by averaging over all the non-equivalent nuclei

Model	Proton pair	$10^3 S_{00}^{(3)}$	$10^3 S_{20}^{(3)}$	$10^3 S_{40}^{(3)}$	Angle between methylene pair and *c* axis
Yokouchi *et al.* model	Aromatic	0.946 1.035	1.440 1.586	0.577 0.639	–
	Outer paraffinic	6.252 6.008	−3.467 −3.500	3.947 2.628	79.5°
	Central paraffinic	7.114 6.617	0.234 0.609	−6.221 −3.827	54.9°
Hall-Pass model 6	Aromatic	0.862 0.762	1.310 1.076	0.537 0.414	–
	Outer paraffinic	8.023 7.901	−6.294 −7.136	7.745 7.434	89.6°
	Central paraffinic	9.277 8.777	−4.922 −4.511	1.901 3.115	75.4°
Hall-Pass model 7	Aromatic	0.872 0.723	1.304 1.036	0.484 0.303	–
	Outer paraffinic	8.375 8.127	−5.933 −7.162	6.914 6.087	86.3°
	Central paraffinic	9.780 8.825	−3.480 −2.510	−4.876 −1.685	66.4°

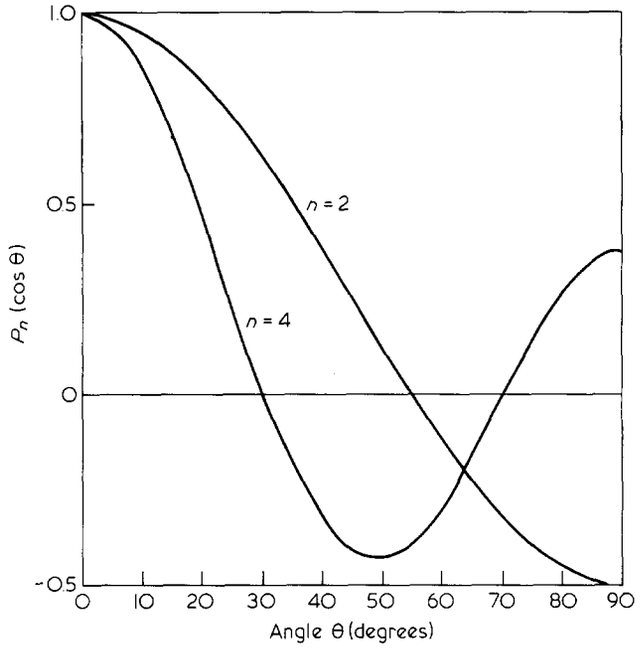

Figure 5 Legendre polynomials P_2 (cos θ) and P_4 (cos θ) as a function of θ

CONCLUSIONS

Broad line nuclear magnetic resonance has shown itself to be very sensitive to small changes in conformation, especially when a group of strongly interacting dipoles, in this case the tetramethylene groups, are well separated by a more weakly interacting group of dipoles, in this case the terephthaloyl residue. This is especially so in a conformation which is practically all *trans* and it is this property which enabled model (7) by Hall and Pass to be identified as the structure which best fits the nuclear magnetic resonance measurements made on β 4GT. In the case of α 4GT, it appears that none of the models proposed to date are in good agreement with the nuclear magnetic resonance measurements and that the cause of this discrepancy originates in the conformation of the centre of the methylene chain.

ACKNOWLEDGEMENTS

We wish to thank Dr T. Smith for supplying the oriented α 4GT tape and the University of Leeds Computing Service for advice and computing facilities. One of us (I.S.D.) is indebted to the Science and Engineering Research Council for the award of a maintenance grant.

REFERENCES

1 Boye, C. A., Jr. and Overton, J. R. *Bull. Am. Phys. Soc. Ser. 2*, 1974, **19**, 352
2 Jakeways, R., Ward, I. M., Wilding, M. A., Hall, I. H., Desborough, I. J. and Pass, M. G. *J. Polym. Sci., Polym. Phys. Edn.* 1975, **13**, 799
3 Jakeways, R., Smith, T., Ward, I. M. and Wilding, M. A. *J. Polym. Sci., Polym. Lett. Edn.* 1976, **14**, 41
4 Brereton, M. G., Davies, G. R., Jakeways, R., Smith, T. and Ward, I. M. *Polymer* 1978, **19**, 17
5 Mencik, Z. *J. Polym. Sci., Polym. Phys. Edn.* 1975, **13**, 2173
6 Hall, I. H. and Pass, M. G. *Polymer* 1976, **17**, 807
7 Desborough, I. J. and Hall, I. H. *Polymer* 1977, **18**, 825
8 Hall, I. H. A.C.S. Symp. Ser. 141, 1980, p 335
9 Yokouchi, M., Sakakibara, Y., Chatani, Y., Tadakaro, H., Tanaka, T. and Yoda, K. *Macromolecules* 1976, **9**, 266
10 Stambaugh, B. D., Koenig, J. L. and Lando, J. B. *J. Polym. Sci., Polym. Lett. Edn.* 1977, **15**, 299
11 Stambaugh, B. D., Koenig, J. L. and Lando, J. B. *J. Polym. Sci., Polym. Phys. Edn.* 1979, **17**, 1053
12 Ward, I. M. and Wilding, M. A. *Polymer* 1977, **18**, 327
13 Kashawagi, M., Cunningham, A., Manuel, A. J. and Ward, I. M. *Polymer* 1973, **14**, 111
14 McBrierty, V. J. and Ward, I. M. *Br. J. Appl. Phys.* 1968, **1**, 1529
15 Davies, G. R., Smith, T. and Ward, I. M. *Polymer* 1980, **21**, 221
16 Davenport, R. A. and Manuel, A. J. *Polymer* 1977, **18**, 557
17 Andrew, E. R. *Phys. Rev.* 1953, **91**, 425
18 Ward, I. M. *J. Polym. Sci.: Polym. Symp.* 1977, **58**, 1